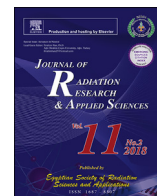


HOSTED BY



Contents lists available at ScienceDirect

Journal of Radiation Research and Applied Sciences

journal homepage: <http://www.elsevier.com/locate/jrras>

Numerical analysis with experimental comparison in duct flow using optimized heat sinks



Kumru Güreşçi ^a, Faruk Yeşildal ^{b,*}, Altuğ Karabey ^c, Rıdvan Yakut ^d, Kenan Yakut ^e

^a Natural Sciences Institute, Mechanical Engineering Department, Uludağ University, 16120, Bursa, Turkey

^b Department of Mechanical Engineering, Faculty of Engineering, Agri Ibrahim Cecen University, 04100, Agri, Turkey

^c Department of Machinery and Metal Technology, Ercis Vocational High School, Yüzüncü Yıl University, 65400, Van, Turkey

^d Department of Mechanical Engineering, Faculty of Engineering and Architecture, Kafkas University, 36100, Kars, Turkey

^e Department of Mechanical Engineering, Faculty of Engineering, Atatürk University, 25100, Erzurum, Turkey

ARTICLE INFO

Article history:

Received 4 April 2017

Received in revised form

1 August 2017

Accepted 30 October 2017

Available online 10 November 2017

Keywords:

Finned heat sink

Electronic cooling systems

Computational Fluid Dynamics (CFD)

ABSTRACT

In many industrial applications, heat must be transferred in the form of either an energy input into the system or removal of energy produced in the system. In this study, heat transfer and flow characteristics of hexagonal finned heat sinks which optimized according to the Taguchi experimental $L_{18}(2^{1*3}7)$ design method in channel flow was analyzed numerically. Ansys-Fluent Icepak module was used in CFD analysis. The analysis carried out for two hexagonal finned optimized heat sinks in 3 different fin heights and 5 different flow velocities. Nusselt number increased with increasing Reynolds number for OH-1 and OH-2 heat sinks with all fin heights. Also, results showed that the friction factor decreased with increasing Reynolds number for all fin heights. According to CFD results, Nu-Re and f-Re variations were obtained and compared with experimental results. The experimental results and the numerical results were quite consistent.

© 2017 The Egyptian Society of Radiation Sciences and Applications. Production and hosting by Elsevier B.V. This is an open access article under the CC BY-NC-ND license (<http://creativecommons.org/licenses/by-nc-nd/4.0/>).

1. Introduction

Electronic systems which have multiple heat-generating parts will have cooling problems. It is especially hard for computer motherboards to achieve needed heat diffusion rates limited interior spaces are densely packed that pose an obstacle to the free circulation of the cooling air (Zhang, Huang, Li, & Chua, 2002). These components behave as strong regional heat sources which should cause high local superheating with heavy power consumption. For this reason effective heat transfer is required for a safe long-lived operation (Niceno, Dronkers, & Hanjalic, 2002).

Today, not only investment costs but also operating costs and lifetime must consider when designing a heat sink. So efficiency of heat sink is the most important parameter. The heat sinks having high effectiveness enhance heat transfer. Thermal conditions must be taken into consideration for effective heat transfer. If this condition is

not satisfied, the maximum junction temperature exceed the allowed temperature by the producing company. So device performance, lifetime and safety may be reduced (Remsburg, 2001).

The heat transfer enhancement methods are classified as active and passive methods in the literature. Those which require external power to maintain the enhancement mechanism are named active methods. On the other hand, the passive enhancement methods are those which do not require external power to sustain the enhancements' characteristics.

At the passive methods, various geometries are designed for effective heat transfer. In general, increment the heat sink surface area reduces the junction temperature of the system. Today, heat sinks are produced for consumer requests in high-tech countries.

CFD (Computational Fluid Dynamics) is a branch of fluid mechanics that based on numerical analysis and algorithms to solve problems that involve fluid flows.

* Corresponding author.

E-mail addresses: gkumru@msn.com.tr (K. Güreşçi), fayesildal@agri.edu.tr (F. Yeşildal), akarabey@yuu.edu.tr (A. Karabey), ryakut@kafkas.edu.tr (R. Yakut), kyakut@atauni.edu.tr (K. Yakut).

Peer review under responsibility of The Egyptian Society of Radiation Sciences and Applications.

Experimental and theoretical methods are two basic approaches to the design of engineering systems. In the first of these, heat and flow characteristics are determined experimentally for produced heat sink model in wind tunnel. In the second one, heat and flow characteristics are obtained by numerical solutions of governing differential equations. Today, engineers use effectively both experimental and CFD analysis.

Tahat et al., studied heat transfer with orthogonal pin-fin which were arranged staggered and in-line in steady-state condition. They determined optimum length between the fins in spanwise and streamwise directions with the given conditions. Nusselt-Reynold variations were investigated with pin-fin pitch (in both directions). Also, they designated that the average heat transfer coefficient increases with increasing Reynolds number (Tahat, Kodah, Jarrah, & Probert, 2000).

Tanda et al., were performed heat transfer and pressure drop with arrays of diamond-shaped elements in rectangular channel. In this studies, the average Nusselt correlations were found to depend on the Reynolds number for each fin configurations. Heat transfer was enhanced by a factor of until 4.4 for uniform mass flow rate and by a factor of until 1.65 for uniform pumping power over diamond-shaped elements (Tanda, 2004).

Lee and Garimella investigated laminar convective heat transfer for uniform wall temperature and axially uniform wall heat flux thermal boundary conditions in the entrance region of rectangular micro channels. They have compared their correlations with other conventional and available experimental correlations. They indicated that their theoretical results are in good agreement with the others (Lee & Garimella, 2006).

Yakut et al., conducted a pioneering experimental study to determine optimum design parameters of hexagonal fins using Taguchi experimental design method (Yakut, Alemdaroglu, Sahin, & Celik, 2006).

2. Materials and methods

In this study, heat transfer and fluid flow characteristics were determined numerically in channel flow for 2 optimized hexagonal finned heat sinks which are coded Optimum Hexagonal-1 (OH-1) and Optimum Hexagonal-2 (OH-2) respectively. ANSYS Icepak was used for numerical analysis. The analyses were performed for 3 different fin heights and 5 different flow velocities for each model. According to CFD results, Nu-Re and f-Re variations were presented and compared with experimental results which are previously obtained (Güreşçi, 2014).

Geometry and mesh of hexagonal finned heat sinks which were optimized according to the Taguchi experimental $L_{18}(2^1 \cdot 3^7)$ design method (Ross, 1989) in channel flow were created.

Two different models which are optimized previous studies (Yakut, Alemdaroglu, Sahin, & Celik, 2006) are used in numerical analysis. The heat sinks were optimized using Taguchi experimental-design method. Optimization criteria are used “the bigger the better” for Nusselt number and “the smaller the better” for friction factor and thermal resistance. Optimization of the heat sinks was based on the channel hydraulic diameter and taking into consideration three objectives. Optimum results were obtained at 150 mm fin height, 14 mm fin span, 20 mm fins distance in cross-stream, 20 mm fins distance in downstream and 4 m/s fluid velocity when Nusselt number calculated for the hexagonal finned heat sinks. The analysis were carried out for 3 different fin heights (100, 150, 200 mm) and 5 different flow velocities (1.2, 2.3, 3.5, 4.2, 4.6 m/s) for each model. Nu-Re and f-Re variations were obtained from the CFD results and the compared with experimental results which are previously obtained (Yesildal, 2007) (see Figs. 1 and 2; Table 1).

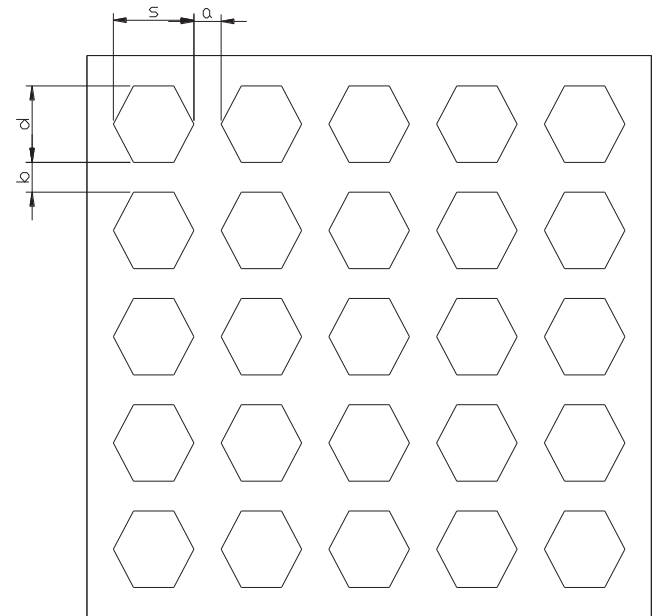


Fig. 1. The general characteristics of the heat sinks.

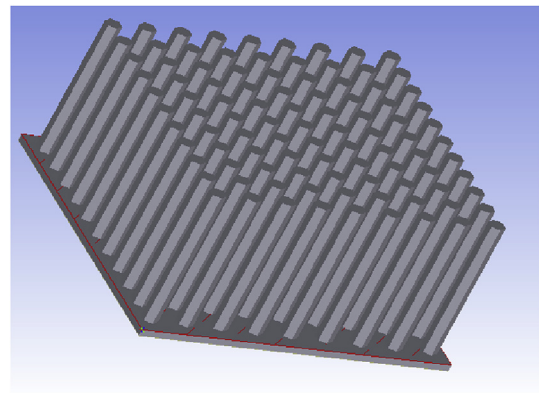


Fig. 2. The perspective view of the hexagonal test model.

Table 1
Parameters in experimental and numerical analysis.

Parameters	Optimal Heat Sink	
	OH-1	OH-2
A Fin span, d[mm]	14	14
B Distance between fins along cross-stream, a[mm]	20	20
C Distance between fins along downstream, b[mm]	20	10

2.1. Calculations of the heat transfer and friction factors

The steady-state rate of the heat transfer through the air can be expressed as follows:

$$Q_{total} = Q_{conv} + Q_{rad} + Q_{cond} \quad (1)$$

$$\dot{Q}_{conv} = \dot{m}c_p(T_{out} - T_{in}) = \frac{V^2}{R} = VI \quad (2)$$

The heat transfer from the test section by convection can also be expressed as;

$$\dot{Q}_{conv} = h_{ave} A_s \left(T_{y,ave} - \frac{T_{out} + T_{in}}{2} \right) \quad (3)$$

Both base plate and fins were made of aluminum: their surfaces were fully cleaned and polished also, working temperature was not too high. So, radiative heat loss is less than 5% of the total input to the pin-fin arrays. For this reason, the radiative heat-loss could be neglected. Using these findings, together with the fact that the section was well insulated and temperature readings of the thermocouple placed at the outer surface of the heating section were nearly equal to ambient temperature, one could assume, with some confidence, that the last two terms of Equation (1) may be ignored. These assumptions are simplified in Equation (1) as follows:

$$\dot{Q}_{total} = \dot{Q}_{conv} \quad (4)$$

Average heat transfer coefficient is obtained from Equations (1)–(3) as follows:

$$h_{ave} = \frac{Q_{conv}}{A_s \left[T_{s,ave} - \left(\frac{T_{out} + T_{in}}{2} \right) \right]} \quad (5)$$

Either the projected or the total area of the test surface can be taken as the surface area in the calculations. These two areas can be related to each other by:

Total area = Projected area + Total surface area contribution from the blocks

$$A_s = WL + n(6eh_k) \quad (6)$$

where W is the width of the base plate, L its length, n the number of fins, e the edge and h_k the height of the hexagonal fins, respectively.

The dimensionless groups are calculated as follows:

$$Nu = \frac{h_{ave} D_h}{k} \quad (7)$$

$$f = \frac{\Delta P}{\rho U_{ave}^2} \left(\frac{D}{L} \right) \quad (8)$$

ΔP , ρ , U_{ave} , U_0 , D , L are named pressure difference, air density, average velocity, velocity at the channel center, hydraulic diameter, channel length, respectively in the above Equation (8). The average velocity of the channel is calculated as follows:

$$U_{ave} = 0,817U_0 \quad (9)$$

The Reynolds number is defined by using eq. (10),

$$Re = \frac{\rho_a U_{ave} D}{\mu} \quad (10)$$

The following steps were applied creating model, creating mesh, solution of the problem (selection of the equation, iteration, error analysis), respectively in the numerical analysis.

2.2. Computational analysis

2.2.1. About Ansys-Icepak procedure

Ansys Icepak has set a standard for speed, precision and ease of use for its electronic cooling features. Reduces the need for physical prototypes by estimating fluid flow and heat transfer at the circuit board or system level.

Ansys Icepak software automatically generates highly accurate meshes from the rough and ladder-step approaches to represent the shape of the unique electronic components. Mesh algorithms

produce multi-block and unstructured hex-dominant meshes that distribute the mesh to solve the fluid boundary layer correctly. The mesh flexibility of Ansys Icepak software results in the fastest solution possible without sacrificing precision.

Ansys Icepak software includes Ansys Fluent, the most advanced technology for thermal and flow calculations. The CFD solver solves all models of heat transfer, including simulations of fluid flow and conduction, convection, radiation, both steady state and transient thermal flow. Solvent uses a multigrid scheme to accelerate solution convergence of complex combined heat transfer problems.

Ansys Icepak software includes sophisticated physical models that can reliably calculate fluid flow and heat transfer calculations since their simulation estimates are accurate and reliable. The software includes advanced thermal modeling features such as contact resistance modeling, periodic boundaries, anisotropic conductivity, and non-linear fan curves along with a number of popular k-epsilon turbulence models (Fabbri, 2011).

Table 2 shows the Icepak outputs for optimum heat sinks. The analysis was carried out at 100, 150 and 200 mm fin heights.

3. Results and discussion

In this study, numerical analysis of the previous experimental study was conducted. Fin height, flow velocity and fin width are amongst the most effective parameters on heat transfer and friction factor of finned surfaces. It was observed that the most efficient two parameters on heat transfer of finned heat sinks were the fin height (h) and flow rate (v ; Re), respectively. Therefore, numerical analyses were performed for optimum hexagon (OH-1 and OH-2) at 3 different fin lengths (100, 150, 200 mm) and 5 different flow rates (1.2, 2.3, 3.5, 4.2, 4.6 m/s) and the results obtained were compared to the experimental results. Numerical and experimental results were found to overlap.

3.1. Variation of Nusselt number with Reynolds number

According to the results of the experimental studies with optimum hexagonal heat sinks Nusselt number increased with increasing Reynolds number and decreased with increasing fin height for OH-1. The highest Nusselt number was observed at a fin height of 100 mm.

The numerical analyses results also showed that Nusselt number increased with increasing flow rate and decreased with increasing fin height.

When analyzed the results of numerical analyses, the highest Nusselt number for OH-1 was found at 100 mm fin height. The Nusselt number increased to 90 percent between the minimum and maximum flow rates for 100 mm fin height. For the same fin height, the average increment in the Nusselt number is between 13–17%. The Nusselt number increased to 84 percent between the minimum

Table 2
Icepak mesh outputs.

	OH1			OH2		
	H = 100	H = 150	H = 200	H = 100	H = 150	H = 200
NUM.ELEMENTS	726,326	711,364	701,824	727,109	702,844	704,284
NODES	759,008	742,508	735,471	759,003	735,511	753,511
HEXAS	721,122	703,920	693,376	720,364	692,664	691,224
PENTAS	5096	7336	8448	6576	9712	12,592
PYRAS	60	60		76	252	252
TETRAS	48	48		93	216	216
QUADS	78,219	80,633	87,004	80,385	88,464	92,144
TRIS	496	496	576	725	928	928
FACES + SOLIDS	25	25	25	25	25	25

and maximum flow rates for 150 mm fin height. For the same fin height, the average increment in the Nusselt number was between 17–19%. Approximately similar values were obtained for 200 mm fin height. Considering the effect of the fin the maximum Nusselt number was obtained for 100 mm fin height for the same Reynolds number. Increment of the Nusselt numbers which calculated for minimum and maximum Reynolds numbers were 17–20%, 14–8% and 33–18% for fin heights between 150–100 mm, 200–150 mm and 200–100 mm, respectively (see Fig. 3).

In both experimental and numerical study the Nusselt number increased with increasing Reynolds number for OH-1 heat sink with 100 mm fin height. The experimental value is 3.61% higher than the numerical value for the first Reynolds number. The difference for following Reynolds numbers are 7.73%, 1.32%, 1.28% and 2.95%, respectively.

In both experimental and numerical study the Nusselt number increased with increasing Reynolds number for OH-1 heat sink with 150 mm fin height. The experimental value is 16.62% higher than the numerical value for the first Reynolds number. The difference for following Reynolds numbers are 19.94%, 16.12%, 12.65% and 17.01%, respectively.

In both experimental and numerical study the Nusselt number increased with increasing Reynolds number for OH-1 heat sink with 200 mm fin height. The experimental value is 4.62% higher than the numerical value for the first Reynolds number. The difference for following Reynolds numbers are 6.25%, 5.59%, 3.7% and 4.92%, respectively (see Figs. 4–6).

According to the results of the experimental studies with optimum hexagonal heat sinks Nusselt number increased with increasing Reynolds number and decreased with increasing fin height for OH-2. The highest Nusselt number was observed at a fin height of 100 mm.

The numerical analyses results also showed that Nusselt number increased with increasing flow rate and decreased with increasing fin height.

When analyzed the results of numerical analyses, the highest Nusselt number for OH-1 was found at 100 mm fin height. The Nusselt number increased to 90 percent between the minimum and maximum flow rates for 100 mm fin height. For the same fin height, the average increment in the Nusselt number is between 20–16%. The Nusselt number increased to 88 percent between the minimum and maximum flow rates for 150 mm fin height. For the same fin height, the average increment in the Nusselt number was between

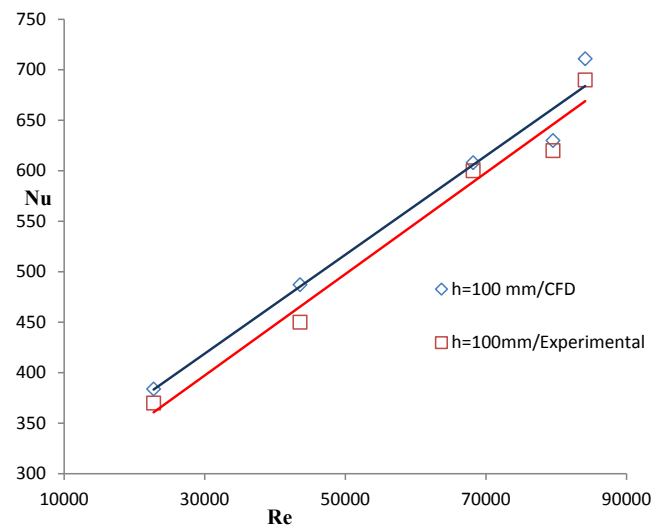


Fig. 4. Comparison of the numerical and experimental results for OH-1 with h = 100 mm.

30–26%. Approximately similar values were obtained for 200 mm fin height. Considering the effect of the fin the maximum Nusselt number was obtained for 100 mm fin height for the same Reynolds number. Increment of the Nusselt numbers which calculated for minimum and maximum Reynolds numbers were 39–34%, 35–39% and 65–70% for fin heights between 150–100 mm, 200–150 mm and 200–100 mm, respectively.

In both experimental and numerical study the Nusselt number increased with increasing Reynolds number for OH-2 heat sink with 100 mm fin height. The numerical value is 9.65% higher than the experimental value for the first Reynolds number. The difference for following Reynolds numbers are 4.57%, 9.14%, 10.57% and 10.28%, respectively (see Figs. 7 and 8).

In both experimental and numerical study the Nusselt number increased with increasing Reynolds number for OH-2 heat sink with 150 mm fin height. The numerical value is 8.34% higher than the experimental value for the first Reynolds number. The difference for following Reynolds numbers are 2.05%, 10.4%, 9.84%, and 11.4%, respectively (see Fig. 9).

In both experimental and numerical study the Nusselt number

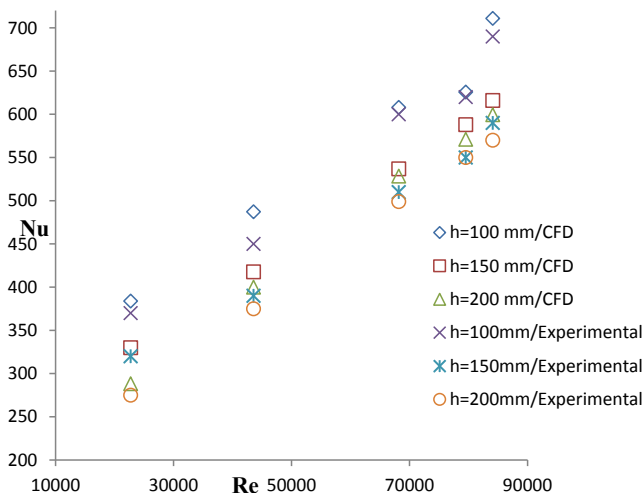


Fig. 3. Comparison of the numerical and experimental results for OH-1.

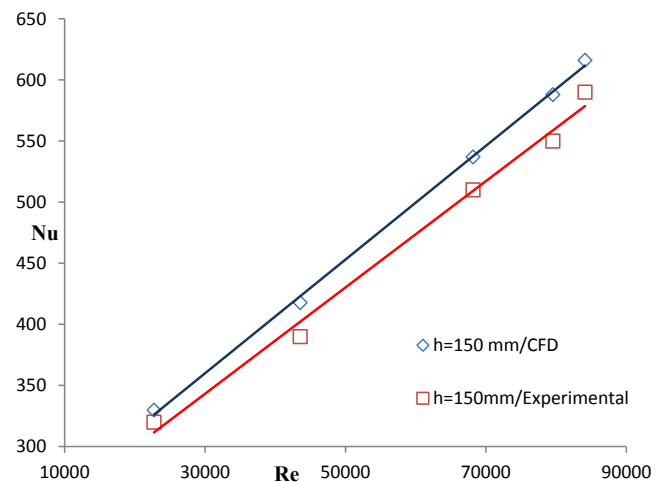


Fig. 5. Comparison of the numerical and experimental results for OH-1 with h = 150 mm.

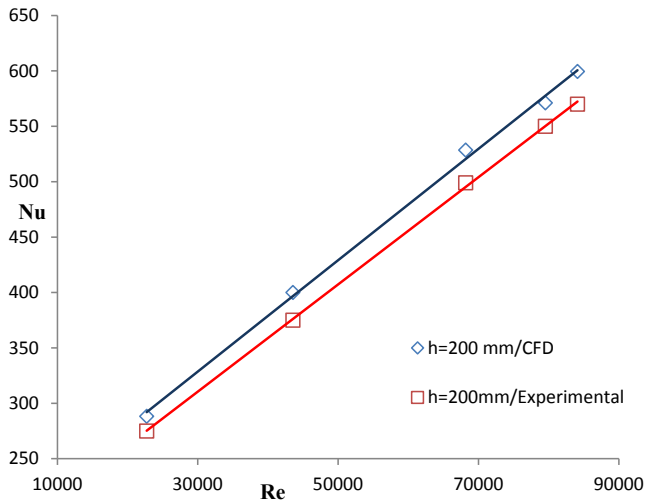


Fig. 6. Comparison of the numerical and experimental results for OH-1 with $h = 200$ mm.

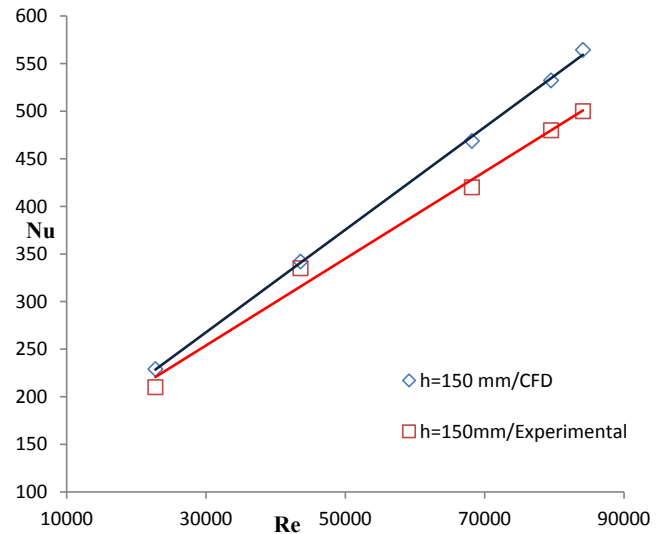


Fig. 9. Comparison of the numerical and experimental results for OH-2 with $h = 150$ mm.

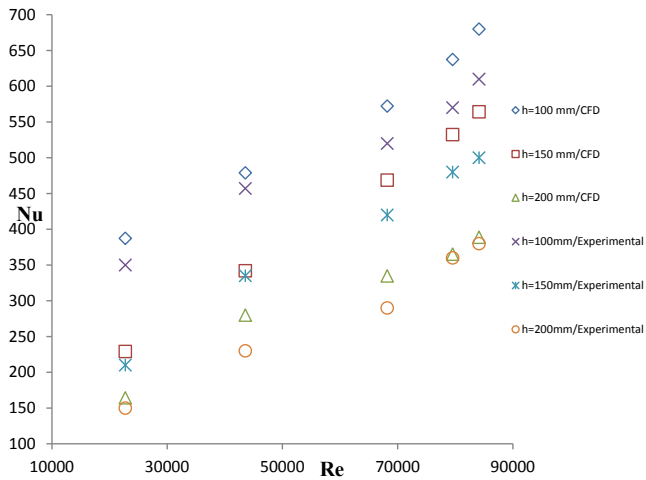


Fig. 7. Comparison of the numerical and experimental results for OH-2.

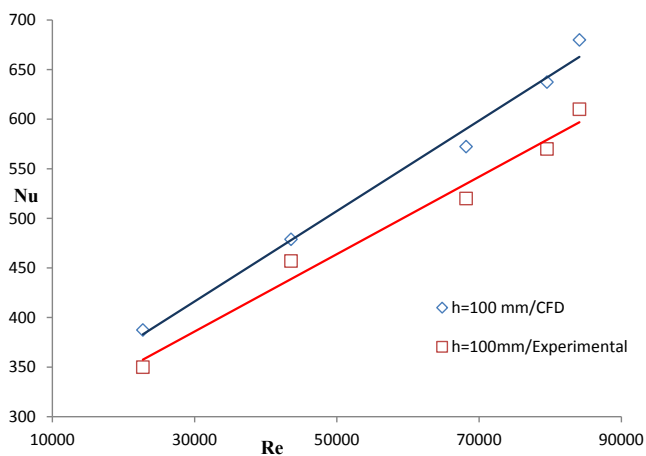


Fig. 8. Comparison of the numerical and experimental results for OH-2 with $h = 100$ mm.

increased with increasing Reynolds number for OH-2 heat sink with 200 mm fin height. The numerical value is 8.67% higher than the experimental value for the first Reynolds number. The difference for following Reynolds numbers are 17.82%, 13.36%, 1.41% and 2.25%, respectively (Fig. 10).

3.2. Variation of friction factor (f) with Reynolds number

According to the results of the experimental studies with optimum hexagonal heat sinks, friction factor decreased with increasing Reynolds number and increased with increasing fin height. The highest friction factor was observed at a fin height of 200 mm and the lowest flow rate.

The numerical analyses results also showed that friction factor decreased with increasing flow rate and increased with increasing fin height. In addition to these, it was observed that the change of friction factor is negligible for the Reynolds number values above 50,000.

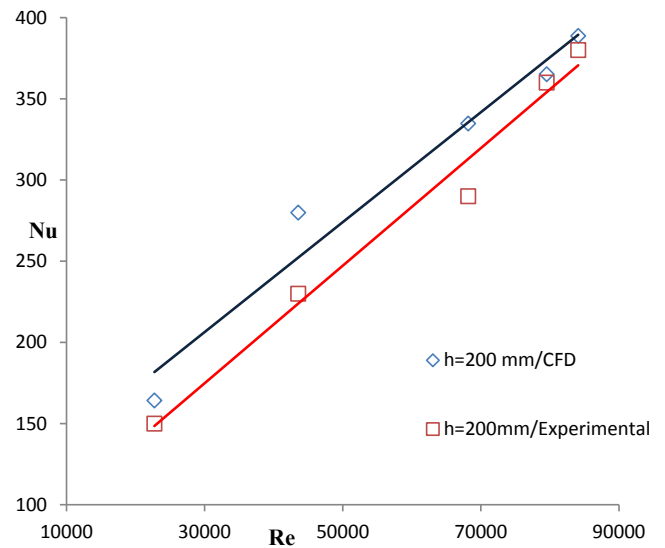


Fig. 10. Comparison of the numerical and experimental results for OH-2 with $h = 200$ mm.

When analyzed the results of numerical analyses, the highest friction factor for OH-1 was found at 200 mm fin height. The friction factor decreased to 73 percent between the minimum and maximum Reynolds number for 200 mm fin height. The friction factor decreased to 71 percent between the minimum and maximum flow rates for 150 mm fin height. The friction factor decreased to 70 percent between the minimum and maximum flow rates for 100 mm fin height.

In both experimental and numerical study the friction factor decreased with increasing Reynolds number for OH-1 heat sink with 100 mm fin height. The numerical value is 1.34% lower than the experimental value for the first Reynolds number. The decrement for following Reynolds numbers are 2.96%, 4.15%, 4.30% and 4.61%, respectively (see Figs. 11 and 12).

In both experimental and numerical study the friction factor decreased with increasing Reynolds number for OH-1 heat sink with 150 mm fin height. The numerical value is 1.31% lower than the experimental value for the first Reynolds number. The decrement for following Reynolds numbers are 2.89%, 3.38%, 3.75% and 4.28%, respectively (Fig. 13).

In both experimental and numerical study the friction factor decreased with increasing Reynolds number for OH-1 heat sink with 200 mm fin height. The numerical value is 1.04% lower than the experimental value for the first Reynolds number. The decrement for following Reynolds numbers are 2.99%, 3.11%, 3.66% and 3.72%, respectively (see Fig. 14).

When analyzed the results of numerical analyses, the highest friction factor for OH-2 was found at 200 mm fin height. The friction factor decreased to 73 percent between the minimum and maximum Reynolds number for 200 mm fin height. The friction factor decreased to 64 percent between the minimum and maximum flow rates for 150 mm fin height. The friction factor decreased to 52 percent between the minimum and maximum flow rates for 100 mm fin height.

In both experimental and numerical study the friction factor decreased with increasing Reynolds number for OH-2 heat sink with 100 mm fin height. The numerical value is 2.36% lower than the experimental value for the first Reynolds number. The decrement for following Reynolds numbers are 4.15%, 4.26%, 4.83% and 4.85%, respectively (see Figs. 15 and 16).

In both experimental and numerical study the friction factor decreased with increasing Reynolds number for OH-2 heat sink with 150 mm fin height. The numerical value is 1.53% lower than

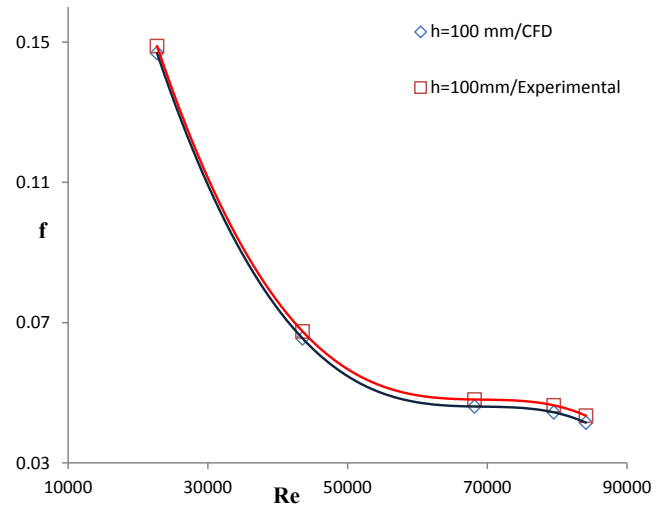


Fig. 12. Comparison of the numerical and experimental results for OH-1 with h = 100 mm.

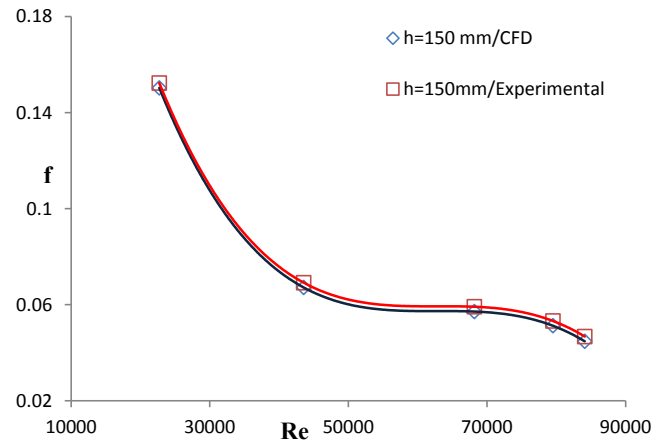


Fig. 13. Comparison of the numerical and experimental results for OH-1 with h = 150 mm.

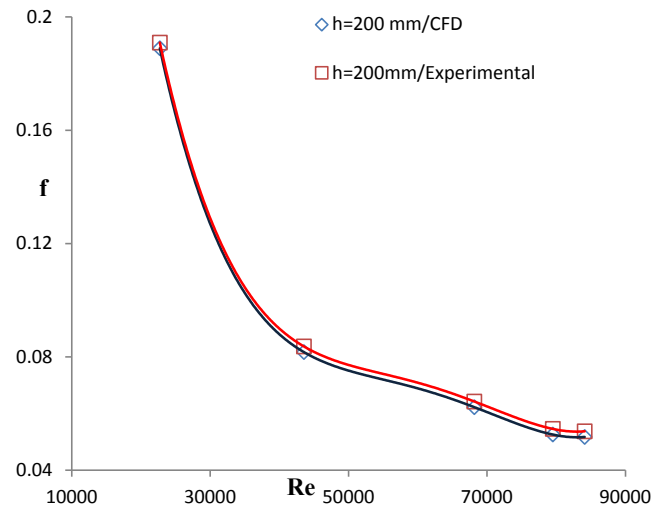


Fig. 14. Comparison of the numerical and experimental results for OH-1 with h = 200 mm.

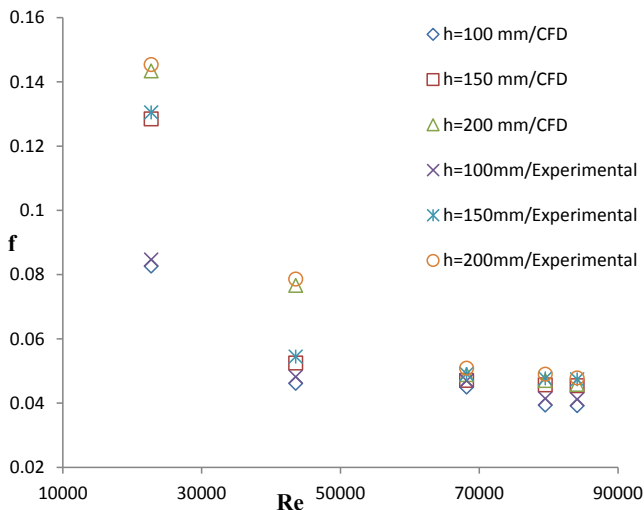


Fig. 11. Comparison of the numerical and experimental results for OH-1.

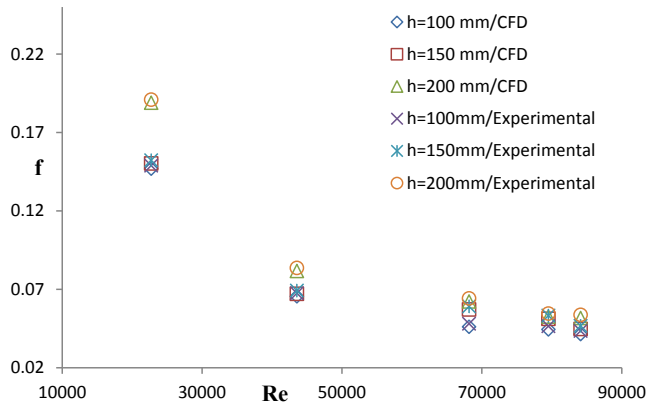


Fig. 15. Comparison of the numerical and experimental results for OH-2.

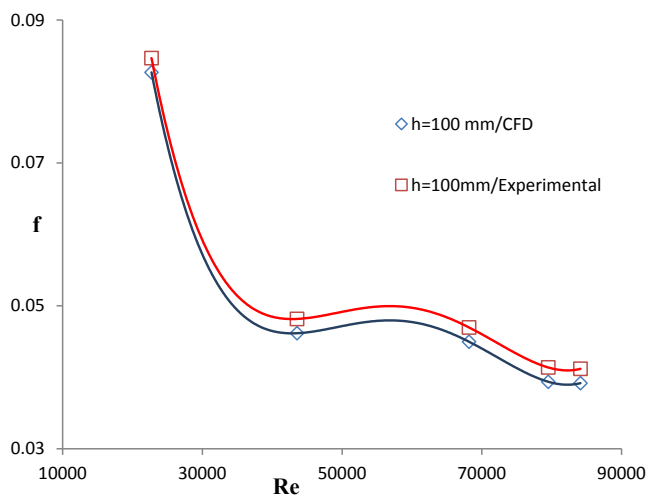


Fig. 16. Comparison of the numerical and experimental results for OH-2 with h = 100 mm.

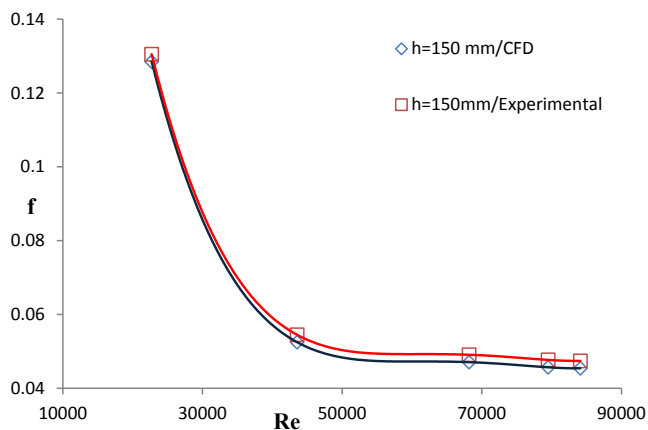


Fig. 17. Comparison of the numerical and experimental results for OH-2 with h = 150 mm.

the experimental value for the first Reynolds number. The decrement for following Reynolds numbers are 3.7%, 4.07%, 4.19% and 4.22%, respectively (Fig. 17).

In both experimental and numerical study the friction factor decreased with increasing Reynolds number for OH-2 heat sink with 200 mm fin height. The numerical value is 1.38% lower than the experimental value for the first Reynolds number. The decrement for following Reynolds numbers are 2.54%, 3.93%, 4.07% and 4.18%, respectively (see Fig. 18).

3.3. Evaluation of mesh quality control

ANSYS Icepak will show a histogram of the skewness, as shown in Fig. 19. Skewness values close to 1 are parallel to the cell quality. Skewness is one of the primary quality measures for a mesh. Skewness determines how close to ideal. According to the definition of skewness, a value of 1 indicates an equilateral cell (best) and a value of 0 indicates a completely degenerate cell. (see Table 3). Our skewness values are in Fig. 19, which is in the close to 1. As you can see, the skewness values are close to 1. This can be interpreted as the quality of the mesh is very good.

The skewness value is calculated as follows:

$$skewness = \frac{cell\ size}{optimum\ cell\ size} \tag{11}$$

4. Conclusions

In this study, heat transfer and fluid flow characteristics were determined numerically in channel flow for experimentally optimized hexagonal heat sinks. The results obtained from the numerical analysis are summarized as follows.

- It was observed that Nusselt number increase and dimensionless friction factor (f) decreases for the OH-1 heat sink with increasing Reynolds number.
- Nusselt number increased with increasing Reynolds number for OH-1 and OH-2 heat sinks with all fin heights.
- It was found that friction factor decreased with increasing Reynolds number for OH-1 and OH-2 hexagonal heat sinks for all fin heights.
- The experimental results and the numerical results were quite consistent.

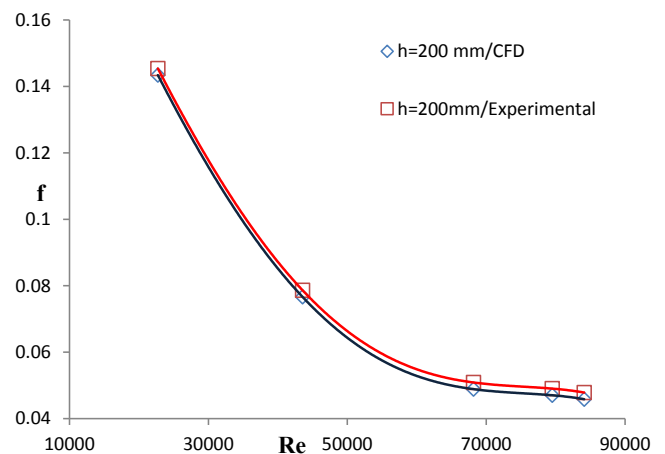


Fig. 18. Comparison of the numerical and experimental results for OH-2 with h = 200 mm.

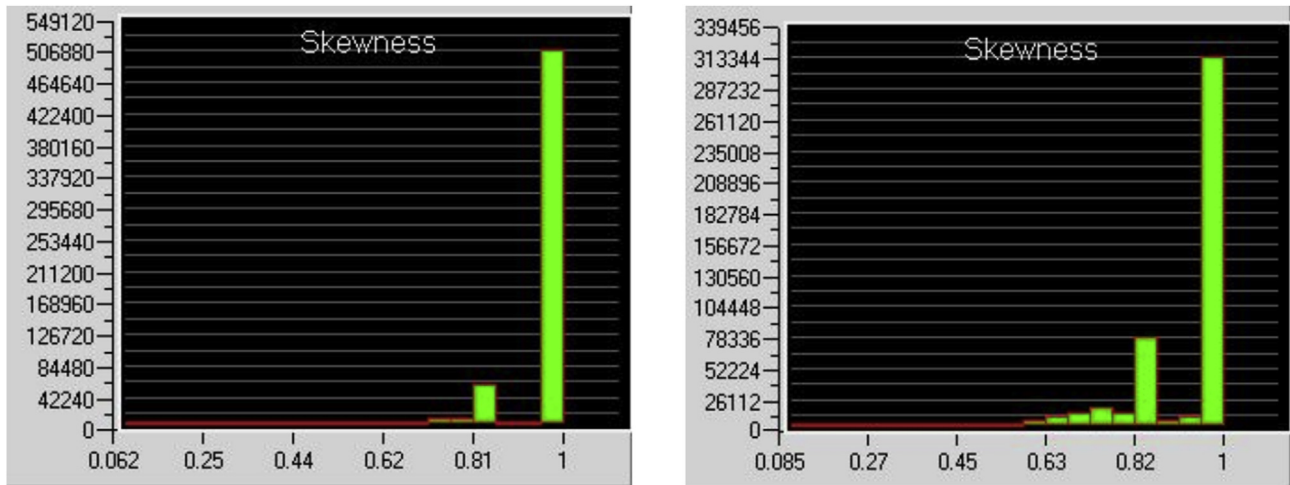


Fig. 19. Icepak skewness histogram.

Table 3
Skewness ranges and cell quality.

Value of skewness	Cell Quality
0	degenerate
<0.02	bad
0.25–0.02	poor
0.5–0.25	fair
0.75–0.5	good
0.75–1	excellent
1	equilateral

Funding

This work was supported by Ataturk University, Research Project Foundation (project number BAP-2011/408).

Nomenclature

A	area, m^2
C_p	pressure coefficient, $J\ kg^{-1}\ K^{-1}$
D	nozzle diameter, m
D_h	hydraulic diameter, m
h	convection coefficient, $W\ m^{-2}\ K^{-1}$
h_k	fin height, m
f	friction factor, dimensionless
I	current, A
k	conduction coefficient, $W\ m^{-1}\ K^{-1}$
l	station distance, m
L	length of the base plate, m
n	total number of fins
e	edge of the base plate, m
\dot{m}	mass flow rate, $kg\ s^{-1}$
Nu	Nusselt number, dimensionless
P	pressure, Pa
Re	Reynolds number, dimensionless
R	resistance, Ω
T	temperature, K
U	velocity, $m\ s^{-1}$
V	potential, V
W	width of the base plate, m

Greek symbols

ϵ	dissipation rate, dimensionless
μ	dynamic viscosity, $kg\ m^{-1}\ s^{-1}$
ρ	density, $kg\ m^{-3}$

Subscripts

a	air
ave	average
cond	conduction
conv	convection
in	inlet
k	fin
out	outlet
rad	radiation
s	surface
tot	total

References

- Fabbri, M., <http://www.ansys.com>, 2011. <http://www.ansys.com/media/ansys/corporate/resourcelibrary/brochure/ansys-icepak-brochure-140.pdf>.
- Güreşçi, K. (2014). Numerical analysis of heat and flow characteristics in duct flow for heat sinks. Erzurum: Atatürk University.
- Lee, P. S., & Garimella, V. (2006). Thermally developing flow and heat transfer in rectangular microchannels of different aspect ratios. *International Journal of Heat and Mass Transfer*, 49(17), 3060–3067.
- Niceno, B., Dronkers, A. D. T., & Hanjalic, K. (2002). Turbulent heat transfer from a multi-layered wall-mounted cube matrix: A large eddy simulation. *International Journal of Heat and Fluid Flow*, 23, 173–185.
- Remsburg, R. (2001). *Thermal design of electronic equipment*. Boca Raton: CRC Press LLC.
- Ross, P. (1989). *Taguchi techniques for quality engineering*. Singapore: McGraw-Hill.
- Tahat, M., Kodah, Z. H., Jarrah, B. A., & Probert, S. D. (2000). Heat transfers from pin-fin arrays experiencing forced convection. *Applied Energy*, 67(4), 419–442.
- Tanda, G. (2004). Heat transfer in rectangular channels with transverse and V-shaped broken ribs. *International Journal of Heat and Mass Transfer*, 47(2), 229–243.
- Yakut, K., Alemdaroglu, N., Sahin, B., & Celik, C. (2006). Optimum design-parameters of a heat exchanger having hexagonal fins. *Applied Energy*, 83, 82–98.
- Yakut, K., Alemdaroglu, N., Sahin, B., & Celik, C. (2006). Optimum design-parameters of a heat exchanger having hexagonal fins. *Applied Energy*, 83(2), 82–98.
- Yesildal, F. (2007). *Experimental and theoretical analysis of heat and flow characteristics in rectangular and hexagonal heat sinks*. Erzurum: Atatürk University.
- Zhang, H., Huang, X. Y., Li, H. S., & Chua, L. P. (2002). Flow patterns and heat transfer enhancement in low-Reynolds-Rayleigh-number channel flow. *Applied Thermal Engineering*, 22(12), 1277–1288.